Full Paper
doi.org/10.1002/chem.202003584

Materials Science |*Hot Paper*|

Interface Amorphization of Two-Dimensional Black Phosphorus upon Treatment with Diazonium Salts

Aleksandra Mitrović[+],[a, b] Stefan Wild[+],[a] Vicent Lloret,[a] Michael Fickert,[a] Mhamed Assebban,[a, c] Bence G. Márkus,[d, e] Ferenc Simon,[d] Frank Hauke,[a] Gonzalo Abellán,*[a, c] and Andreas Hirsch*[a]

Abstract: Two-dimensional (2D) black phosphorus (BP) represents one of the most appealing 2D materials due to its electronic, optical, and chemical properties. Many strategies have been pursued to face its environmental instability, covalent functionalization being one of the most promising. However, the extremely low functionalization degrees and the limitations in proving the nature of the covalent functionalization still represent challenges in many of these sheet architectures reported to date. Here we shine light on the structural evolution of 2D-BP upon the addition of electrophilic diazonium salts. We demonstrated the absence of covalent functionalization in both the neutral and the reductive routes, observing in the latter case an unexpected interface conversion of BP to red phosphorus (RP), as characterized by Raman, ^{31}P-MAS NMR, and X-ray photoelectron spectroscopies (XPS). Furthermore, thermogravimetric analysis coupled to gas chromatography and mass spectrometry (TG-GC-MS), as well as electron paramagnetic resonance (EPR) gave insights into the potential underlying radical mechanism, suggesting a Sandmeyer-like reaction.

Introduction

Since its renaissance in 2014 black phosphorus (BP) has brought in many exciting opportunities to the 2D materials research field, such as a tunable direct band gap, high charge carrier mobility and optical anisotropy.[1] Bulk BP has a layered graphitic-like structure, however, with the P atoms being sp^3 hybridized (instead of sp^2 in graphene), each bearing a lone pair of electrons thus forming a puckered lattice. The outstanding properties of this 2D material may impact future electronics technologies, although its environmental instability still represents the main hurdle in BP research.[2] To date, the problem of BP degradation under ambient conditions has been addressed by several strategies that can roughly be divided into two groups: noncovalent and covalent functionalization of the BP surface. The noncovalent approach offers physical protection of BP against water and oxygen by applying a range of passivation layers.[3] It has been recently reported that, beyond suppressing the degradation of BP, covalent functionalization offers the possibility to fine-tune the chemical and physical properties of the material.[4] However, the extremely low functionalization degrees obtained through the neutral route using diazonium salts, as well as more than possible dimerization/polymerization of the molecules make it very difficult to draw accurate conclusions about this covalent functionalization strategy.[5,6] Due to this fact, an unambiguous determination of the covalent binding became quite difficult. Facing these challenges, we have recently reported the covalent modification of 2D BP via a reductive route employing negatively charged BP.[7] Alkali metal BP intercalation compound (BPIC) was allowed to react with alkyl iodides and subsequent NMR results

[a] *Dr. A. Mitrović,[+] S. Wild,[+] V. Lloret, M. Fickert, Dr. M. Assebban, Dr. F. Hauke, Dr. G. Abellán, Prof. A. Hirsch*
Chair of Organic Chemistry II and Joint Institute of Advanced Materials and Processes (ZMP), Friedrich-Alexander-Universität Erlangen-Nürnberg (FAU), Nikolaus Fiebiger-Strasse 10, 91058 Erlangen and Dr.-Mack Strasse 81, 90762 Fürth (Germany)
E-mail: andreas.hirsch@fau.de
gonzalo.abellan@fau.de

[b] *Dr. A. Mitrović[+]*
Faculty of Chemistry, University of Belgrade
Studentski trg 12–16, 11000 Belgrade (Serbia)

[c] *Dr. M. Assebban, Dr. G. Abellán*
Instituto de Ciencia Molecular (ICMol), Universidad de Valencia
Catedrático José Beltrán 2, 46890 Paterna (Spain)

[d] *Dr. B. G. Márkus, Prof. F. Simon*
Department of Physics, Budapest University of Technology and Economics and MTA-BME Lendület Spintronics Research Group (PROSPIN), PO Box 91, 1521 Budapest (Hungary)

[e] *Dr. B. G. Márkus*
Wigner Research Centre for Physics
Institute for Solid State Physics and Optics
1121 Budapest (Hungary)

[+] *These authors contributed equally to this work.*

Supporting information and the ORCID identification number(s) for the author(s) of this article can be found under: https://doi.org/10.1002/chem.202003584.

indicate that the BPIC contains roughly 7% of localized and negatively charged P atoms that reacted quantitatively in a substitution reaction to form a P–C bonds. After functionalization, the corresponding P-atoms do not form phosphonium sites but rather P–P bond breakage takes place, leading to lattice opening and the formation of phosphine centres. Herein, we report about the exploration of the functionalization sequence with the first step being a single electron transfer (SET) from the negatively charged BPIC to the high energy electrophile (E). With this strategy, we targeted the question of whether it is possible to obtain a high degree of covalent functionalization with diazonium salts, which are expected to be much more reactive than the alkyl halides whose successful addition we have accomplished previously.[7] We were also interested in the comparison with the same reaction employing non-activated neutral BP. For this purpose, we have selected three phenyldiazonium tetrafluoroborate salts **D1–3** (Figure 1) bearing different substituents in *para* position (and therefore having disparate Hammet constants and reduction potentials), to react with K/Na intercalated BP. To confirm the difference between the reactivity of pristine BP and KP_6/NaP_6, all reactions were complemented by corresponding control experiments, more precisely a neutral route reaction in which pristine BP was allowed to react with the respective diazonium salts **D1–3**. As a result of these studies we can conclude that both the neutral and the reductive approaches using diazonium salts do not lead to covalent functionalization, and in the case of BPICs induces amorphization of the interface.

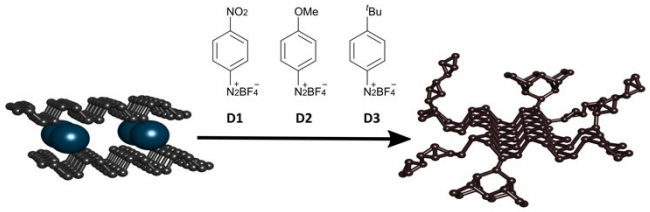

Figure 1. The reaction of intercalated BP with diazonium salts **D1–D3** leading to an amorphous reaction product.

Results and Discussion

The BP functionalization reactions with the three phenyldiazonium tetrafluoroborate salts **D1–3** (Figure 1) were carried out under strictly inert conditions using an argon-filled glovebox and thoroughly purified solvents (see Supporting Information). In particular, the BPICs (1 mmol, 1 equiv)—prepared according to the previously reported procedure[8]—were suspended in THF (30 mL) using an ultrasonication tip (5 min) yielding the respective phosphenide suspensions. Subsequently, diazonium salts **D1–3** (1 mmol, 1 equiv) were added to the phosphenide suspensions and the reaction mixtures were stirred for 24 h. The reaction products were isolated by vacuum filtration, followed by thorough washing using THF. The same experimental settings were used for the neutral route, obviously with the addition of a liquid phase exfoliation step before the functionalization.

Covalent functionalization of neutral BP with diazonium salts **D1–3** afforded dark grey powders whose Raman fingerprint corresponds to the pristine black phosphorus spectrum, with no additional peaks characteristic for the P–C bond (see Supporting Information, Figure S1). Related TGA-MS analysis reveals a mass loss around the temperature of 450 °C and only mass fragments characteristic for unmodified BP (m/z = 31, 62, 93, and 124) were observed (see Supporting Information, Figure S2). Also, a quantitative magic angle spinning ^{31}P solid state nuclear magnetic resonance (^{31}P MAS NMR) experiments showed the expected band for phosphorene at 18.2 ppm without any additional signals (see Supporting Information, Figure S3). Once again, these observations highlight the necessity to activate BP with alkali metals to achieve the desired covalent modification, even if highly reactive reagents like diazonium salts are used. When adding diazonium salts to the suspension of K/Na BPICs the reaction mixture immediately turns reddish and the colour change is followed by nitrogen gas release. Based on these observations one could assume that an arylation reaction is taking place. However, the characterization of the reaction products by Raman spectroscopy revealed the existence of pristine BP together with the appearance of the characteristic fingerprints of red phosphorus (RP) (Figure 2). The presence of a red-coloured powder along with BP crystals can even be distinguished with an optical microscope. Moreover, crystalline RP has a polymeric structure that can be viewed as a derivative of P4 where covalent bonds are formed between the neighbouring tetrahedra, resulting in a chain-like structure. Due to its thermodynamic instability, RP usually exists as an amorphous intermediate phase.[9] Amorphous RP (a-RP) consists of P4 and P9 cages arranged to form pentagonal tubes in paired layers.[10] In the Raman spectral region between 300–540 cm^{-1} a-RP exhibits eleven vibrational peaks, although not all can be resolved (Figure 2b).[9,11] The most specific and intense peak can be seen at around 350 cm^{-1} and P9 cages are considered to be responsible for its appearance. The obtained Raman spectrum of the reaction product of KP_6 with **D3** (Figure 2a) clearly shows the presence of the peaks corresponding to pristine BP (362 cm^{-1}, 439 cm^{-1}, 467 cm^{-1}). These signals are closely accompanied by signals originating from RP, often merging into a plateau of non-resolved peaks, with one isolated low intensity peak at 505 cm^{-1}, which is believed to be associated with the A1 symmetric stretch of the P4 structure. These results are in accordance with recently reported Raman spectra for BP/RP-quantum dots heterostructures.[12] The Raman spectra of all three products suggest a mixture of a-RP and BP, regardless of the type of the substituent on the aromatic core.

Additionally, we explored the reaction of the nitrobenzene derivative **D1**, which is the most reactive one, with BPICs of different alkali metal loadings, generated by varying the Na stoichiometric ratio (Na:P) from 1:10 to 1:1 (see SI, Figure S4). We observed no impact of the type of alkali metal (Na/K) on the overall compositions of the products. However, the amount of intercalated metal. seems to be directly related to the volume

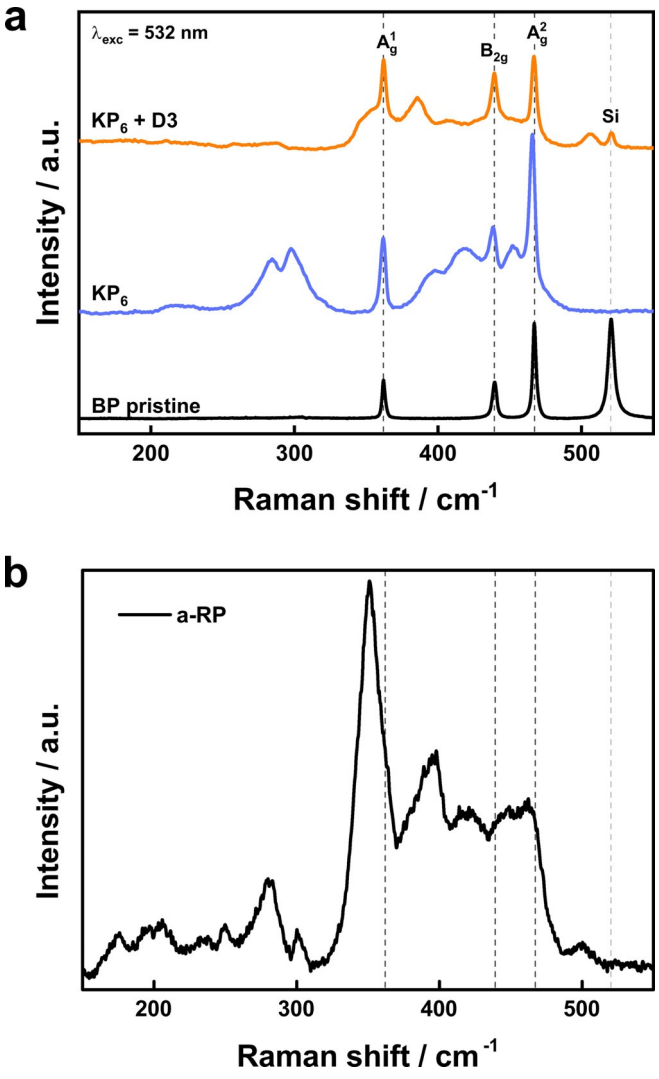

Figure 2. a) Raman spectroscopy monitoring the reaction of KP_6 with **D3** using an excitation wavelength of $\lambda_{exc} = 532$ nm. Raman spectra of the final product are dominated by the broad peak between 340 cm^{-1} and 470 cm^{-1} and one isolated low intensity peak at 505 cm^{-1}. b) Mean Raman spectra of commercially available pristine red P, usually labelled as "type 1".

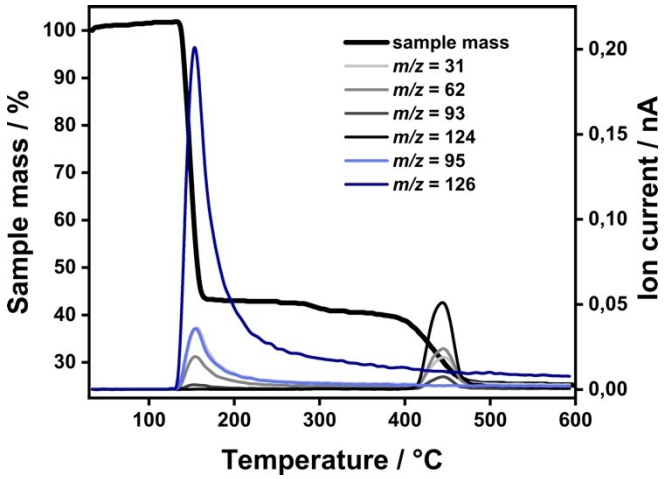

Figure 3. TG-MS analysis of the reaction product of KP_6 with **D2**. The obtained TG curve displays a significant mass loss at 160 °C which can be correlated to the decomposition of 1-fluoro-4-metoxybenzene before the BP/RP lattice decomposes to P4 and P4-based clusters (m/z = 31, 62, 93 and 124). Related signals of the ion current for the detection of fluoro-derivative are m/z = 95 and 126. The slight increase observed below 160 °C is related to an instrumental inaccuracy during the tare process due to the low amount of sample.

of the amorphous structures in the reaction products. The formation of a-RP is facilitated when the amount of the alkali metal is increased.

The reaction product of KP_6 with **D1** was further investigated by NMR, [^{1}H-^{31}P] cross-polarization mode was used to acquire the spectrum, there was only one signal emerging at 18.2 ppm, which corresponds to pristine BP. This indicates that the BP lattice remains unaltered, in terms of covalent functionalization because no specific signals for the formation of phosphine or phosphonium species were detected.[7]

To further evaluate the nature of the obtained products, we performed a thermogravimetric analysis coupled with mass spectrometry (MS). The resulting TG profiles, obtained upon heating up to 600 °C, clearly show that a complete mass loss of the sample is happening in a multistep process, in contrast to the neutral ones (see Supporting Information, Figures S6, S7). In Figure 3 an example is illustrated for the reaction of KP_6 with **D2**. First, a major mass loss of about 60% occurs already at approximately 160 °C. Related mass spectra reveal the detection of the characteristic mass fragments for the phenyl-cation/radical (m/z = 39, 51, 65, 77), which could suggest the presence of the aryl functionalization (see Supporting Information, Figure S5). Second, another mass loss is observed above 400 °C and can be explained by the complete decomposition of BP to P4 and P4-based clusters (m/z = 31, 62, 93, 124).

To elucidate the chemical structure of the molecules related to the first step of the mass loss, we performed TG/MS analysis combined with gas chromatography (see SI, Figures S8, S9), a very powerful technique previously used in covalently functionalized graphene.[13] In the case of treatment with **D2**, the sample was heated to 600 °C and the gaseous fragments that evolved at 160 °C were separated by a GC column. The obtained elugram revealed a peak at 8.3 min of retention time, which corresponds to 1-fluoro-4-methoxybenzene, as unambiguously revealed by MS. These data confirm our hypothesis that the fluorination of an aryl radical is promoted by the counter ion of the diazonium salt and takes place instead of a P–C bond formation. Furthermore, we performed an X-ray photoelectron spectroscopy (XPS). As shown in Figure 4 b, two peaks at about 130.1, and 130.9 eV are present which correspond to the P $2p_{3/2}$, and P $2p_{1/2}$ core level, respectively. Again, no sign of covalent modification in terms of the formation of a P–C bond is observed. Hence, the question arises, why does the use of very reactive diazonium compounds such as electrophiles cause these drastic changes in the Raman spectrum without yielding any covalent functionalization. The most reasonable explanation is the formation of radical centres on the P-lattice due to single electron transfer (SET) from the BPIC to the diazonium compound. First of all, to confirm the presence of itinerant charge carriers (or excess electrons) in our reaction sequence, electron paramagnetic resonance (EPR) measure-

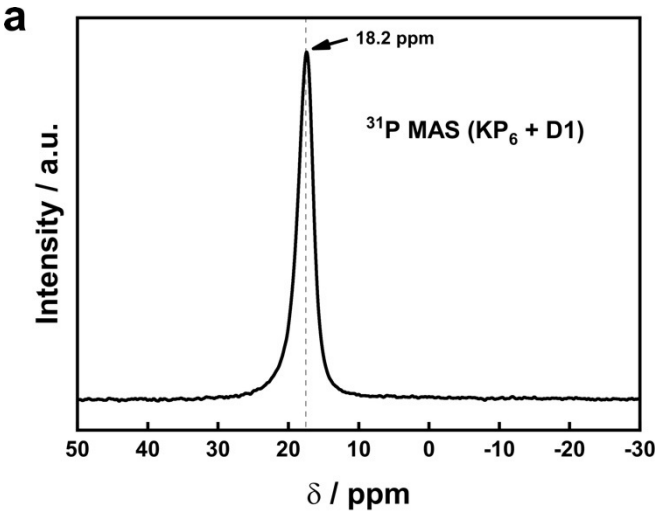

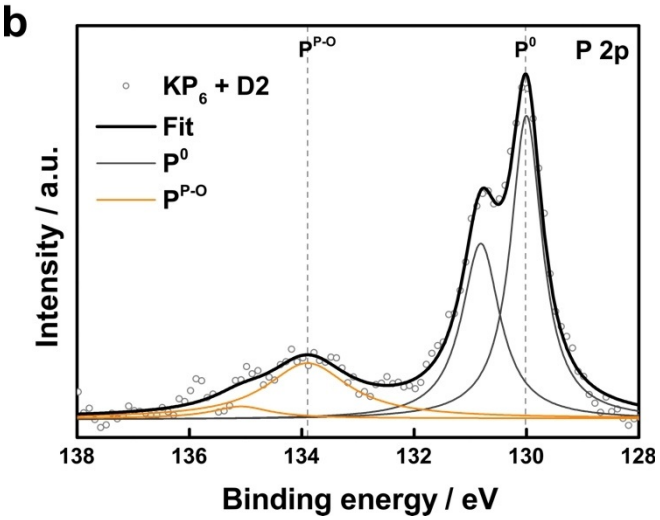

Figure 4. a) ^{31}P MAS NMR spectrum of the reaction product of intercalated BP (KP_6) + D1 showing only one signal at 18.2 ppm, which can be assigned to pristine BP; b) XPS spectrum of the reaction product of KP_6 + D2 displaying the P 2p region. Besides the P^0 species and the minor contribution of P^{P-O}, no obvious contribution of a P^{P-C} species can be found.

ments were conducted. Indeed, EPR studies of metal intercalated BP reveals the presence of negative charges on P atoms, thus indicating a partial radical character of the BPIC (see Supporting Information, Figure S10). Subsequently, negatively charged BP sheets are expected to display reactive behaviour towards radical reactions. Radical addition mechanism leads to the formation of an aryl radical and a phosphorus radical that should react to form a P–C bond. However, phosphorus radicals in the basal plane of BP are highly unstable due to the lack of steric hindrance and p–π conjugation, therefore the BP lattice undergoes a fast destruction and bond reorientation instead of an addition.[14] This is in contrast to the nucleophilic substitution reaction when adding an alkyl iodide to a BPIC. There, the intercalation of BP is necessary to activate the relatively chemically inert 2D towards nucleophilic addition. Based on the observations that the ordered lattice of BP is rather decomposing to the lower degree of organization than it is

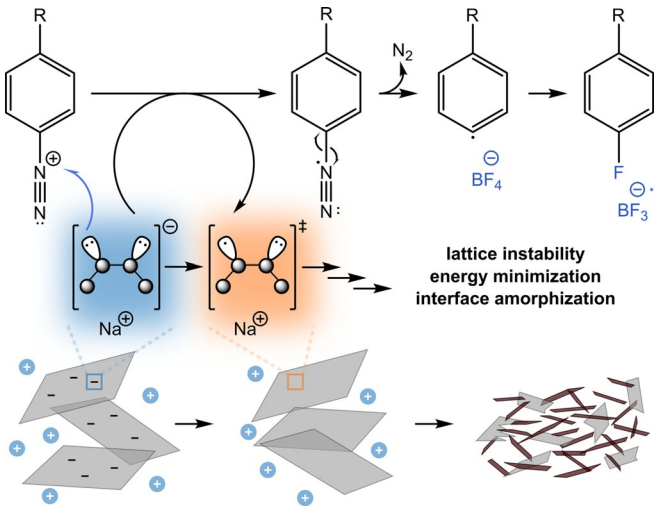

Figure 5. Proposed mechanism of Sandmeyer's-type reaction leading to a Baltz–Schiemann product, with BPIC having a role of sacrificial catalyst.

being functionalized, we postulated the mechanism of such alteration. The most probable scenario is that BPIC is acting as a sacrificial catalyst in a reaction such as Sandmeyer's (Figure 5), but leading to a Balz–Schiemann product.[15] The mechanism begins with a SET from the BPIC to the diazonium salt to form a neutral diazo radical. The unpaired electrons at the P atoms in the P-lattice at the same time are highly reactive centres that can give rise to fast structural and morphological changes of the lattice, thus stabilizing the system. The diazo radicals on the other hand release N_2 to form aryl radicals. These radicals can be quenched by termination reactions such as fluorination, dimerization, or polymerization. The different stability of the diazo radicals (**D3** > **D2** > **D1**) determines the rate of these quenching procedures. As a consequence, the variations observed in the TG-MS analysis corroborates this assumption, namely, the characteristic lack of control of diazonium salts, as previously observed for neutral reaction conditions.[4a,5,6] In fact, this is not the first time that a radical reaction has been catalysed by BPICs. It has been proven that BPICS, specifically KP_6, can promote/catalyse the radical addition of haloalkanes to alkenes (showing an easy halide transferring) and with high turnover frequency.[16]

Conclusions

To conclude, we have demonstrated that the addition of diazonium salts to neutral BP and BP intercalation compounds does not lead to covalent functionalization. Instead, in the case of BPICs, it causes a drastic structural evolution in the interface of few-layer BP leading to amorphous RP. This was demonstrated by employing Raman spectroscopy, ^{31}P MAS-NMR spectroscopy, TGA coupled to GC-MS and XPS. Most probably, this process is promoted by intermediate radical centres on the P-lattice, which form after a SET transfer takes place from the BPIC to the diazonium salt. Due to the high amount of unpaired electrons on the BP surface, the lattice undergoes a structural alteration to form amorphous RP-like structures. This work pro-

vides mechanistic insights into the covalent chemistry of BP, which will further help modify this 2D material in a controlled way, allowing its future stabilization under ambient conditions and precise tuning of its electrical properties.

Experimental Section

Materials and functionalization process

For all experiments BP was purchased from Smart Elements with purity higher than 99.999% was used. First, BP crystals were mortared before they were intercalated with potassium/sodium to create KP_6 or NaP_6 following the procedure, which was previously described by our working group.[8] The obtained black phosphorus intercalation compounds (BPICs) were dispersed in purified THF (1 mg mL^{-1}). Ultra-sonication using a Bandelin SONOPULS HD4100 sonotrode for 5 minutes (power amplitude: 25%; time interval: 2 s) yielded a stable dispersion of negatively charged BP layers. In the next step, diazonium salt **D1–3** (Sigma Aldrich) was added as electrophilic functionalization reagent (1 equiv. per phosphorous atom) and the dispersion was stirred for 1 hour before the functionalized BP powder was obtained by filtration. The whole functionalization process was performed in an argon-filled LABmasterpro sp glove box (MBraun) equipped with a gas purifier and solvent vapor removal unit (oxygen and water content lower than 0.1 ppm).

Solvent purification

THF was first dried over molecular sieves with a size of 3 Å for at least 3 days to remove dissolved water. With this step, the water content could be determined utilizing the Karl Fischer method to be lower than 5 ppm. Afterward, the THF was degassed using the Freeze–Pump–Thaw method to remove oxygen, before it was introduced into the glove box. Additionally, the THF was distilled in the glove box over a Na/K alloy to further reduce the water content.

Characterization

Raman spectroscopy: Raman spectra were acquired using a LabRam HR Evolution confocal Raman microscope (Horiba) equipped with an automated XYZ table using 0.80 NA objectives. An excitation wavelength of 532 nm was used preferentially to characterize the covalently functionalized BP. For the better resolution of the spectra, a grating of 1800 grooves mm^{-1} was selected, whereat an acquisition time of 2 s was used. Additionally, the laser intensity was kept below 5% (0.88 mW) to avoid photo-induced laser oxidation of the samples. For all Raman studies the samples were drop casted on a Si/SiO_2 (300 nm oxide layer) substrate.

Thermogravimetric analysis coupled to mass spectrometry: Thermogravimetric analysis was performed on a Netzsch STA 409CD Skimmer equipped with an EI ion source and a quadrupole mass spectrometer. Time-dependent temperature profile: 25–600 °C (10 K min^{-1} temperature ramp) and cooling to 30 °C. The initial sample weights were adjusted at 5.0(±0.1) mg and the whole experiment was executed under an inert gas atmosphere with a He gas flow of 80 mL min^{-1}.

Thermogravimetric analysis (TGA) combined with Fourier-transformed infrared spectroscopy (FT-IR), gas-chromatographic separation (GC) and coupled with a mass spectrometer (MS): Thermogravimetric analysis was carried out on a Perkin–Elmer Pyris 1 TGA instrument. Time-dependent temperature profiles in the range of 20 and 250 °C (10 K min^{-1} gradient) were recorded under a constant flow of N_2 (70 mL min^{-1}). About 2.0 mg of initial sample mass was used. The evolved gases detached from the respective sample in combination with the N_2 carrier gas are transferred into the FT-IR and GC system through a TL9000 TG-IR-GC interface at a constant temperature of 160 °C. Frontier spectrometer equipped with a $LiTaO_3$ MIR detector. The gas-S4 chromatographic separation was achieved by a GC-Clarus 680 with a polysiloxane-coated Elite-5MS capillary column: 30 m length, 0.25 mm diameter, 0.25 μm film thickness. A GC injection fraction of 150 μL was collected at the selected TG temperature (in the 200–300 °C range), parameters: injector zone = 280 °C, detection zone = 250 °C, split = 8.2 mL min^{-1}, flow rate helium = 10 mL min^{-1}, temperature profile = 34 min total run time, dynamic ramp = 24 min, 40–280 °C with a 10 K min^{-1} gradient followed by an isothermal step of 10 min at 250 °C. MS measurements were performed on an MS Clarus SQ8C (multiplier: 1800 V). The obtained data were processed with the TurboMass Software and Bibliographic searches were performed with NIST MS Search 2.0.

Electron paramagnetic resonance (EPR) spectroscopy: EPR spectra were recorded on a commercial Magnettech MS-300 X-band spectrometer equipped with a rectangular TE102 microwave cavity, operated at room temperature. During the measurements, the microwave power was 10 mW. No saturation effects were observed, due to the metallic behaviour of the material. The modulation amplitude was 2 G, which is gradually smaller than the width of the observed lines. The samples were sealed under vacuum in high purity quartz tubes.

X-ray photoelectron spectroscopy: X-ray photoemission (XP) spectra of covalently functionalized and pristine BP were collected at room temperature. Synthesis, preparation, and transfer into the XPS chamber took place in Argon, that is, in an oxygen-free atmosphere. Drop-cast preparation onto unpolished gold foil, which was sonicated in isopropanol for at least 2 min and dried in the air before transfer to Argon atmosphere. The shown data were collected using monochromatized Al Kα radiation. The base pressure of the UHV system was within the low 10^{-10} mbar regime. The pass energy was 10 eV for the acquisition of narrow, high-resolution scans of certain regions of the spectrum, and 50 eV for the acquisition of survey spectra. Unless stated otherwise, the given binding energies are referenced to the Fermi energy of the gold support material, and calibration was done using the binding energy of Au 4f7/2 signals, which was set to be 84.0 eV in accordance to literature. Linear baselines were adjusted to narrow P2p region scans. For the analysis pseudo-Voigt profiles, that is a product of weighted Lorentzian and Gaussian with 40% Gaussian contribution, were fitted to the data.

Acknowledgements

A.H. and G.A. acknowledge the financial support from the European Research Council (ERC Advanced Grant 742145 B-PhosphoChem to A.H., and ERC Starting Grant 2D-PnictoChem 804110 to G.A.) for support. The research leading to these results was partially funded by the European Union Seventh Framework Programme under grant agreement No. 604391 Graphene Flagship. G.A. acknowledges support by the Generalitat Valenciana (CIDEGENT/2018/001and iDiFEDER/2018/061 cofinanced by FEDER), the Spanish MICINN (PID2019-111742GA-I00 and Excellence Unit María de Maeztu (CEX2019-000919-M)), and the Deutsche Forschungsgemeinschaft (DFG, FLAG-ERA AB694/2-1). A.H. and A.G. thank the SFB 953 "Synthetic Carbon

Allotropes" funded by the DFG for support and the Cluster of Excellence "Engineering of Advanced Materials". A.M. thanks Alexander von Humboldt (AvH) Foundation for a postdoctoral fellowship. Support by the National Research, Development, and Innovation Office of Hungary (NKFIH) Grant Nos. K119442 and 2017-1.2.1-NKP-2017-00001 are acknowledged. Open access funding enabled and organized by Projekt DEAL.

Conflict of interest

The authors declare no conflict of interest.

Keywords: amorphization · Balz–Schiemann product · black phosphorus · red phosphorus · sacrificial catalysts

[1] a) X. Ling, H. Wang, S. Huang, F. Xia, M. S. Dresselhaus, *Proc. Natl. Acad. Sci. USA* **2015**, *112*, 4523 – 4530; b) B. Li, C. Lai, G. Zeng, D. Huang, L. Qin, M. Zhang, M. Cheng, X. Liu, H. Yi, C. Zhou, F. Huang, S. Liu, Y. Fu, *Small* **2019**, *15*, 1804565; c) A. Castellanos-Gomez, *J. Phy. Chem. let.* **2015**, *6*, 4280 – 4291; d) J. D. Wood, S. A. Wells, D. Jariwala, K.-S. Chen, E. Cho, V. K. Sangwan, X. Liu, L. J. Lauhon, T. J. Marks, M. C. Hersam, *Nano Lett.* **2014**, *14*, 6964 – 6970; e) L. Li, J. Kim, C. Jin, G. J. Ye, D. Y. Qiu, F. H. da Jornada, Z. Shi, L. Chen, Z. Zhang, F. Yang, K. Watanabe, T. Taniguchi, W. Ren, S. G. Louie, X. H. Chen, Y. Zhang, F. Wang, *Nat. Nanotech.* **2017**, *12*, 21; f) J. Qiao, X. Kong, Z.-X. Hu, F. Yang, W. Ji, *Nat. Commun.* **2014**, *5*, 4475; g) L. Vaquero-Garzon, R. Frisenda, A. Castellanos-Gomez, *Nanoscale* **2019**, *11*, 12080 – 12086; h) W. Xin, H. B. Jiang, T. Q. Sun, X. G. Gao, S. N. Chen, B. Zhao, J. J. Yang, Z. B. Liu, J. G. Tian, C. L. Guo, *Nano Mater. Sci.* **2019**, *1*, 304 – 309.

[2] S. Kuriakose, T. Ahmed, S. Balendhran, V. Bansal, S. Sriram, M. Bhaskaran, S. Walia, *2D Mater.* **2018**, *5*, 032001.

[3] a) G. Abellán, S. Wild, V. Lloret, N. Scheuschner, R. Gillen, U. Mundloch, J. Maultzsch, M. Varela, F. Hauke, A. Hirsch, *J. Am. Chem. Soc.* **2017**, *139*, 10432 – 10440; b) G. Abellán, V. Lloret, U. Mundloch, M. Marcia, C. Neiss, A. Görling, M. Varela, F. Hauke, A. Hirsch, *Angew. Chem. Int. Ed.* **2016**, *55*, 14557 – 14562; *Angew. Chem.* **2016**, *128*, 14777 – 14782; c) Y. Zhao, Q. Zhou, Q. Li, X. Yao, J. Wang, *Adv. Mater.* **2017**, *29*, 1603990; d) V. V. Korolkov, I. G. Timokhin, R. Haubrichs, E. F. Smith, L. Yang, S. Yang, N. R. Champness, M. Schröder, P. H. Beton, *Nat. Commun.* **2017**, *8*, 1385; e) S. Walia, S. Balendhran, T. Ahmed, M. Singh, C. El-Badawi, M. D. Brennan, P. Weerathunge, M. N. Karim, F. Rahman, A. Rassell, J. Duckworth, R. Ramanathan, G. E. Collis, C. J. Lobo, M. Toth, J. C. Kotsakidis, B. Weber, M. Fuhrer, J. M. Dominguez-Vera, M. J. S. Spencer, I. Aharonovich, S. Sriram, M. Bhaskaran, V. Bansal, *Adv. Mater.* **2017**, *29*, 1700152; f) J.-S. Kim, Y. Liu, W. Zhu, S. Kim, D. Wu, L. Tao, A. Dodabalapur, K. Lai, D. Akinwande, *Sci. Rep.* **2015**, *5*, 8989.

[4] a) C. R. Ryder, J. D. Wood, S. A. Wells, Y. Yang, D. Jariwala, T. J. Marks, G. C. Schatz, M. C. Hersam, *Nat. Chem.* **2016**, *8*, 597 – 602; b) Y. Cao, X. Tian, J. Gu, B. Liu, B. Zhang, S. Song, F. Fan, Y. Chen, *Angew. Chem. Int. Ed.* **2018**, *57*, 4543 – 4548; *Angew. Chem.* **2018**, *130*, 4633 – 4638.

[5] Z. Sofer, J. Luxa, D. Bouša, D. Sedmidubský, P. Lazar, T. Hartman, H. Hardtdegen, M. Pumera, *Angew. Chem. Int. Ed.* **2017**, *56*, 9891 – 9896; *Angew. Chem.* **2017**, *129*, 10023 – 10028.

[6] a) M. van Druenen, F. Davitt, T. Collins, C. Glynn, C. O'Dwyer, J. D. Holmes, G. Collins, *Chem. Mater.* **2018**, *30*, 4667 – 4674; b) L. Zhang, L.-F. Gao, L. Li, C.-X. Hu, Q.-Q. Yang, Z.-Y. Zhu, R. Peng, Q. Wang, Y. Peng, J. Jin, H.-L. Zhang, *Mater. Chem. Front.* **2018**, *2*, 1700 – 1706.

[7] S. Wild, M. Fickert, A. Mitrovic, V. Lloret, C. Neiss, J. A. Vidal-Moya, M. Á. Rivero-Crespo, A. Leyva-Pérez, K. Werbach, H. Peterlik, M. Grabau, H. Wittkämper, C. Papp, H.-P. Steinrück, T. Pichler, A. Görling, F. Hauke, G. Abellán, A. Hirsch, *Angew. Chem. Int. Ed.* **2019**, *58*, 5763 – 5768; *Angew. Chem.* **2019**, *131*, 5820 – 5826.

[8] G. Abellán, C. Neiss, V. Lloret, S. Wild, J. C. Chacón-Torres, K. Werbach, F. Fedi, H. Shiozawa, A. Görling, H. Peterlik, T. Pichler, F. Hauke, A. Hirsch, *Angew. Chem. Int. Ed.* **2017**, *56*, 15267 – 15273; *Angew. Chem.* **2017**, *129*, 15469 – 15475.

[9] J. M. Zaug, A. K. Soper, S. M. Clark, *Nat. Mater.* **2008**, *7*, 890.

[10] H. Hartl, *Angew. Chem. Int. Ed. Engl.* **1996**, *34*, 2637 – 2638.

[11] D. J. Olego, J. A. Baumann, M. A. Kuck, R. Schachter, C. G. Michel, P. M. Raccah, *Solid State Commun.* **1984**, *52*, 311 – 314.

[12] R. Shi, F. Liu, Z. Wang, Y. Weng, Y. Chen, *Chem. Commun.* **2019**, *55*, 12531 – 12534.

[13] G. Abellán, M. Schirowski, K. F. Edelthalhammer, M. Fickert, K. Werbach, H. Peterlik, F. Hauke, A. Hirsch, *J. Am. Chem. Soc.* **2017**, *139*, 5175 – 5182.

[14] a) X.-P. Kong, X. Shen, J. Jang, X. Gao, *J. Phys. Chem. Lett.* **2018**, *9*, 947 – 953; b) Z. Yazhuo, M. Yuchen, J. Ran, L. Huichao, Y. Zhijun, *Electron. Struct.* **2020**, *2*, 025005.

[15] a) T. Sandmeyer, *Ber. Dtsch. Chem. Ges.* **1884**, *17*, 1633 – 1635; b) C. G. Swain, R. J. Rogers, *J. Am. Chem. Soc.* **1975**, *97*, 799 – 800.

[16] a) M. Tejeda-Serrano, V. Lloret, B. G. Márkus, F. Simon, F. Hauke, A. Hirsch, A. Doménech-Carbó, G. Abellán, A. Leyva-Pérez, *ChemCatChem* **2020**, *12*, 2126; b) V. Lloret, M. Á. Rivero-Crespo, J. A. Vidal-Moya, S. Wild, A. Doménech-Carbó, B. S. J. Heller, S. Shin, H.-P. Steinrück, F. Maier, F. Hauke, M. Varela, A. Hirsch, A. Leyva-Pérez, G. Abellán, *Nat. Commun.* **2019**, *10*, 509.

Manuscript received: August 1, 2020
Accepted manuscript online: October 13, 2020
Version of record online: January 21, 2021

